Sodium-Independent Low-Affinity D-Glucose Transport by Human Sodium/D-Glucose Cotransporter 1: Critical Role of Tryptophan 561†

Azad Kumar,‡,§ Navneet K. Tyagi,‡,|| Pankaj Goyal,⊥ Dharmendra Pandey,⊥ Wolfgang Siess,⊥ and Rolf K. H. Kinne*,‡

Max Planck Institute of Molecular Physiology, Otto-Hahn Strasse 11, 44227 Dortmund, Germany, and Institute for Prevention of Cardiovascular Disease, Ludwig Maxmilian University, Pettenkoferstrasse 9, 80336 Munich, Germany

Received August 19, 2006; Revised Manuscript Received November 14, 2006

ABSTRACT: Although there is no evidence of significant Na-independent glucose flux in tissues naturally expressing SGLT1, previous kinetic and biophysical studies suggest that sodium/D-glucose cotransporter 1 (hSGLT1) can facilitate sodium-independent D-glucose transport and may contain more than one sugar binding site. In this work, we analyze the kinetic properties and conformational states of isolated hSGLT1 reconstituted in liposomes by transport and fluorescence studies in the absence of sodium. In the transport studies with hSGLT1, significant sodium-independent phlorizin inhibitable α-methyl D-glucopyranoside (α-MDG) uptake was observed which amounted to ∼20% of the uptake observed in the presence of a sodium gradient. The apparent affinity constant for α-MDG was thereby 3.4 ± 0.5 mM, a value ∼10-fold higher than that in the presence of sodium. In the absence of sodium, various sugars significantly decreased the intrinsic Trp fluorescence of hSGLT1 in proteoliposomes exhibiting the following sequence of affinities: α-MDG > D-glucose ≈ D-galactose > 6-deoxy-D-glucose > 2-deoxy-D-glucose > D-allose. Furthermore, significant protection effects of D-glucose or phlorizin against potassium iodide, acrylamide, or trichloroethanol quenching were observed. To locate the Trps involved in this reaction, we generated mutants in which all Trps were sequentially substituted with Phe. None of the replacements significantly affected sodium-dependent uptake. Uptake in the absence of sodium and typical fluorescence changes depended, however, on the presence of Trp at position 561. This Trp residue is conserved in all known SGLT1 forms (except *Vibrio parahaemolyticus* SGLT) and all SGLT isoforms in humans (except hSGLT3). If all these data are taken into consideration, it seems that Trp-561 in hSGLT1 forms part of a low-affinity sodium-independent binding and/or translocation site for D-glucose. The rate of sodium-independent translocation via hSGLT1 seems, however, to be tightly regulated in the intact cell by yet unknown factors.

Sodium/D-glucose cotransporter 1 (SGLT1) of *Homo sapiens*, encoded by the *SGLT1* gene (*1*), catalyzes the intracellular accumulation of D-glucose and D-galactose by utilizing the energy of the Na^+ electrochemical gradients in osmotic work to drive sugar across the membrane (*2*). Extensive molecular biology, biochemical, and biophysical studies of hSGLT1[1] in *Xenopus laevis* oocytes revealed that the N-terminal half of the protein contains the Na^+ binding sites (*3*) while the solute and inhibitor binding sites lie in the C-terminal half of protein (*4*, *5*). Further studies of this topic indicate that residues Gln-457 and Thr-460 (*6*) and a negative charge at residue Asp-454 form part of the sugar binding and translocation pathway (*7*). Recently, recombinant hSGLT1 was expressed and purified from *Pichia pastoris*. Intrinsic Trp fluorescence studies of recombinant hSGLT1 in solution identified three different conformational states of the transporter in solution, one for the empty carrier, one for the sugar−sodium carrier complex, and one for the carrier blocked by phlorizin (*8*). Studies from our group (*9*) using yeast secretory vesicles for the expression of SGLT1 in an inside-out orientation demonstrated that SGLT1 can translocate D-glucose without sodium. The transport of the sugar had a low affinity, was independent of sodium, and was not inhibited by phlorizin. Also, earlier kinetic transport studies by Centelles et al. (*10*) on renal brush border membrane vesicles demonstrated the presence of a low-affinity leak pathway for sugars in the sodium/D-glucose cotransporter where translocation of sugars without sodium could occur (*10*). However, in intact tissues naturally expressing SGLT1,

† This work was supported by funds from the Max Planck Institute of Molecular Physiology. We thank the International Max Planck Research School in Chemical Biology, Dortmund, Germany (NKT), the August-Lenz-Stiftung, and the Deutsche Forschungsgemeinschaft [Graduate Program "Vascular Biology in Medicine" GRK438 (P.G.), SFB 413, and Si 274/9] for support.

* To whom correspondence should be addressed: Max Planck Institute of Molecular Physiology, Otto-Hahn-Str. 11, 44227 Dortmund, Germany. E-mail: rolf.kinne@mpi-dortmund.mpg.de. Telephone: +49 (0) 231-97426491. Fax: +49 (0) 231-97426479.

‡ Max Planck Institute of Molecular Physiology.

§ Present address: Department of Physiology and Biophysics, School of Medicine, University of Colorado at Denver and Health Science Center, Aurora, CO 80045.

|| Present address: Department of Genetics and Howard Hughes Medical Institute, Yale University School of Medicine, New Haven, CT 06510.

⊥ Ludwig Maxmilian University.

[1] Abbreviations: hSGLT1, human sodium/D-glucose cotransporter 1; D-Glu, D-glucose; Phlz, phlorizin; KI, potassium iodide; TCE, trichloroethanol; K_{SV}, Stern−Volmer quenching constant.

10.1021/bi061696x CCC: $37.00
Published on Web 02/09/2007

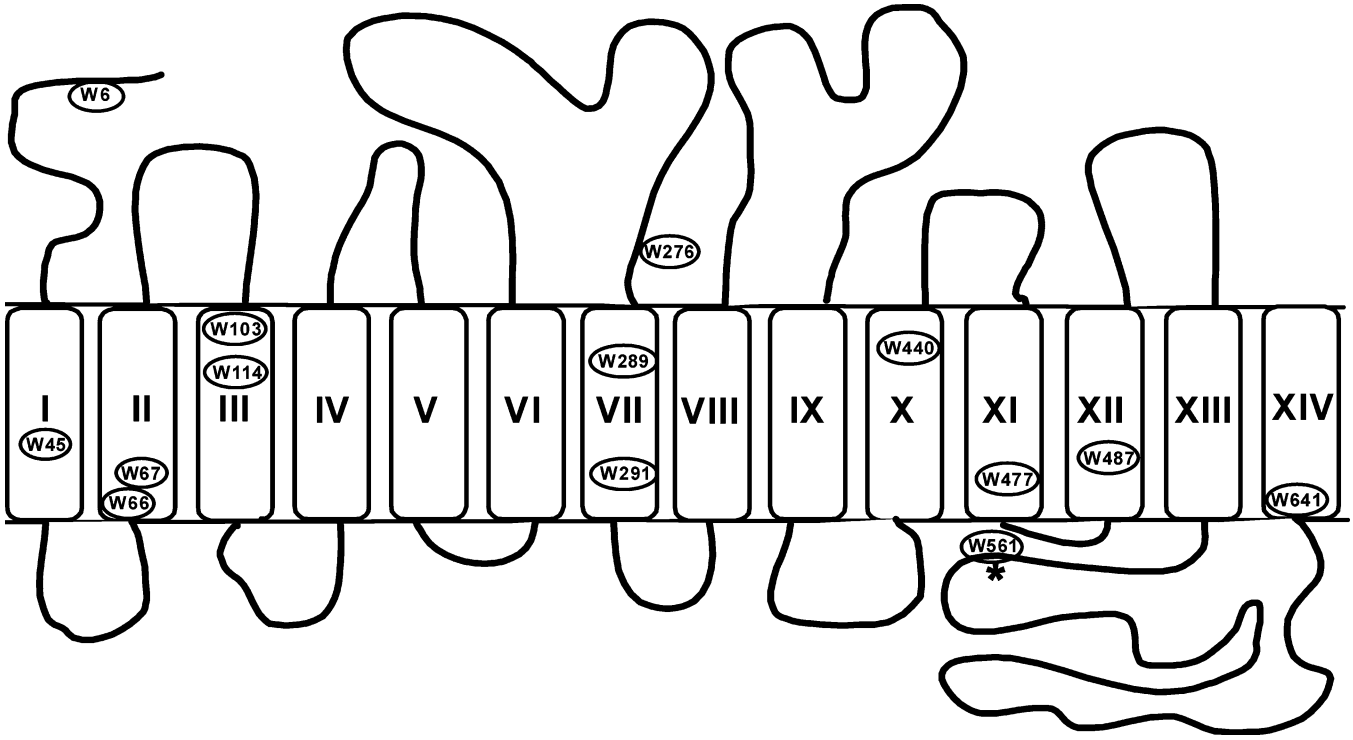

FIGURE 1: Hypothetical two-dimensional topology model of hSGLT1. hSGLT1 consists of 14 α-helical transmembrane domains (columns) with the N- and C-termini located on the extracellular faces of the membrane. Positions of different tryptophan residues are marked with ovals, and Trp-561 is designated with an asterisk.

the level of sodium-independent sugar uptake is usually very low (*11*). As a next step for the identification of such a potential sodium-independent low-affinity sugar binding/translocation site in hSGLT1, we have performed transport and fluorescence studies with recombinant hSGLT1 and with two mutants, W561hSGLT1 containing only a single Trp residue at position 561 and W0hSGLT1 (no Trp residue) reconstituted in proteoliposomes. The results support the notion that at least two sugar binding/translocation sites can be distinguished in isolated hSGLT1, a high-affinity site for D-glucose with a K_d of ~0.5 mM and a low-affinity site with a K_d of 3−4 mM. The latter is sodium-independent and appears to involve Trp at position 561. Thus, in intact cells, mechanisms that strongly control this sugar leakage pathway must be postulated.

EXPERIMENTAL PROCEDURES

Materials. All sugars, phloretin, phlorizin, and trichloroethanol were from Sigma (Munich, Germany). All media (LB, YPD, BMMGY, and BMMY) were from Invitrogen (Carlsbad, CA). α-Methyl D-[^{14}C]glucopyranoside ([^{14}C]-α-MDG) was from Perkin-Elmer LAS (Rodgau-Jügesheim, Germany). All other chemicals were analytical grade and obtained from commercial sources.

Site-Directed Mutagenesis. hSGLT1 contains 14 Trp residues at positions 6, 45, 66, 67, 103, 114, 276, 289, 291, 440, 477, 487, 561, and 641 (Figure 1). Thirteen Trp residues of 14 for W561hSGLT1 (except W561) and all Trps to make W0hSGLT1 were mutated to Phe using the Quick-Change mutagenesis kit (Stratagene, Amsterdam, The Netherlands) in accordance with the manufacturer's protocol. Mutants (underlined) were generated using the following primers: W6F, 5′-GACAGTAGCACCTTTAGCCCCAAGACC-3′ (forward) and 5′-GGTCTTGGGGCTAAAGGTGCTACTGTC-3′ (reverse); W45F, 5′-GCCGTCGGACTGTTT-GCTATGTTTTCC-3′ (forward) and 5′-GGAAAACATAGCAAACAGTCCGACGGC-3′ (reverse); W66F/W67F, 5′-GAAGTATGGTGTTCTTCCCGATTGGAG-3′ (forward) and 5′-CTCCAATCGGGAAGAACACCATACTTC-3′ (reverse); W103F, 5′-GGAGGCTTTGAATTTAATGCCCTGG-3′ (forward) and 5′-CCAGGGCATTAAATTCAAAGCCTCC-3′ (reverse); W114F, 5′-GTTGTGCTGGGCTTTCTGTTTGTCCCC-3′ (forward) and 5′-GGGGACAAACAGAAAGCCCAGCACAAC-3′ (reverse); W276F, 5′-GGAGACCTCCCATTTCCTGGGTTCATC-3′ (forward) and 5′-GATGAACCCAGGAAATGGGAGGTCTCC-3′ (reverse); W289F/W291F, 5′-CCTTACCTTGTTCTACTTCTGCACAGATC-3′ (forward) and 5′-GATCTGTGCAGAAGTAGAACAAGGTAAGG-3′ (reverse); W440F, 5′-ATCAGCATCGCCTTTGTGCCCATTGTG-3′ (forward) and 5′-CACAATGGGCACAAAGGCGATGCTGAT-3′ (reverse); W477F, 5′-GCTATTTTCTTCAAGAGAGTCAATGAG-3′ (forward) and 5′-CTCATTGACTCTCTTGAAGAAAATAGC-3′ (reverse); W487F, 5′-CCAGGAGCCTTTTTTGGACTGATCCTAG-3′ (forward) and 5′-CTAGGATCAGTCCAAAAAAGGCTCCTGG-3′ (reverse); W561F, 5′-TACCGTCTGTGTTTTAGCCTGCGCAAC-3′ (forward) and 5′-GTTGCGCAGGCTAAAACACAGACGGTA-3′ (reverse); and W641F, 5′-GAGAAGCCTTTGTTCAGGACAGTGTTG-3′ (forward) and 5′-CAACACTGTCCTGAACAAAGGCTTCTC-3′ (reverse). For all mutagenesis reactions, the template was wild-type pPICZb-hSGLT1 (*8*). Trp to Phe mutations were confirmed by DNA sequencing.

Protein Expression, Purification, and Reconstitution. Wild-type and all mutants of hSGLT1 were expressed in *P. pastoris*, purified, and reconstituted into proteoliposomes (9:1

asolectin soy lecithin:cholesterol ratio) according to a procedure described in ref *8*.

Transport Studies. Proteoliposomes [preloaded with 100 mM potassium phosphate (pH 7.5) and 2 mM β-mercaptoethanol] were subjected to three sonication−freeze−thaw cycles before uptake assays were conducted at 22 °C. Uptake was initiated by mixing 10 μL of proteoliposomes with 10 μL of transport buffer 2× (200 mM choline chloride, 50 mM NaCl, 100 mM mannitol, 20 mM Tris, 20 mM Hepes, 6 mM $MgSO_4$, and 2 mM $CaCl_2$) in the presence of Na^+ or with 10 μL of transport buffer 2× (200 mM choline chloride, 50 mM KCl, 100 mM mannitol, 20 mM Tris, 20 mM Hepes, 6 mM $MgSO_4$, and 2 mM $CaCl_2$) in the presence of K^+ with α-methyl D-[^{14}C]glucopyranoside ([^{14}C]-α-MDG). Each reaction was stopped with 1 mL of ice-cold stop solution (10 mM Tris, 10 mM Hepes, 100 mM mannitol, 150 mM KCl, 50 mM choline chloride, 50 mM NaCl, 3 mM $MgSO_4$, 1 mM $CaCl_2$, and 0.2 mM phlorizin), applied centrally to a 0.22 μm GSWP nitrocellulose filter (Millipore) over vacuum and washed with 3 mL of ice-cold stop solution, and the filter was assayed by scintillation counting. All experiments were performed in at least triplicate, and errors indicate the standard error of the mean values.

Steady-State Fluorescence Studies and Ligand Binding Assay. All fluorescence experiments reported in this study were performed with hSGLT1 or W561hSGLT1 reconstituted into proteoliposomes (liposomes were composed of a 9:1 asolectin soy lecithin/cholesterol mixture). The final protein concentration was 1 μM, and the lipid:protein molar ratio was 200:1. Steady-state fluorescence measurements were taken with a Perkin-Elmer LS 50B fluorescence spectrometer (Perkin-Elmer), fitted with a 450 W xenon arc lamp at room temperature. A 0.3 cm excitation and emission path length quartz cell was used for all the fluorescence measurements. The excitation wavelength was set to 295 nm for selective excitation of Trp. A 290 nm cutoff filter was used to minimize the contribution of scattering signals. Emission spectra were collected from 320 to 400 nm, with an average of six scans. The bandwidths for both excitation and emission monochromators were 5 nm. The emission spectra were corrected for the liposome blank (scatter) which at the maximal lipid concentration used contributed at most 10% to the total signal, and for the inner-filter effect. The ligand-induced fluorescence quenching as a function of D-glucose (D-Glu), D-galactose (D-Gal), 6-deoxy-D-glucose (6Doglc), 2-deoxy-D-glucose (2Doglc), mannose (Man), allose (All), L-glucose (L-Glc), or phlorizin (Phlz) concentration was monitored, and dissociation constants (K_d) were calculated as described previously (*8*).

Quenching of Intrinsic Protein Fluorescence. Steady-state fluorescence quenching experiments were carried out by measuring the fluorescence intensities at the emission maxima as a function of the quencher concentration. Increasing concentrations of the quencher were added from a concentrated stock solution of the quencher in the same buffer. All quencher solutions were freshly prepared, and 0.1 mM $Na_2S_2O_3$ was added to the KI stock solution to prevent I_3^- formation. The accessibility of Trp was monitored by analyzing the quenching data using a Stern−Volmer equation:

$$F_0/F = 1 + K_{SV}[Q]$$

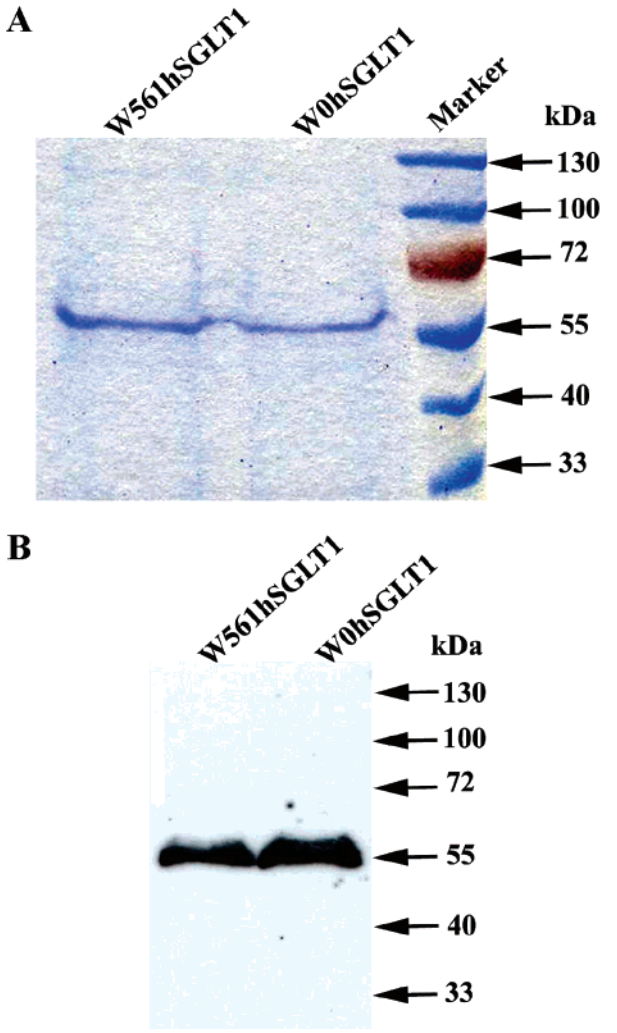

FIGURE 2: Coomassie-stained SDS−PAGE gel and immunoblot of it with an anti-FLAG antibody of purified W0hSGLT1 and W561hSGLT1.

where F_0 and F are the fluorescence intensities in the absence and presence of quencher, respectively, [Q] is the concentration of quenching agent, and K_{SV} is the Stern−Volmer quenching constant. In the case of a purely collisional quenching mechanism, the Stern−Volmer plot of F_0/F versus [Q] is linear with a slope equal to K_{SV}.

RESULTS

Protein Expression and Purification. hSGLT1 contains 14 Trp residues at positions 6, 45, 66, 67, 103, 114, 276, 289, 291, 440, 477, 487, 561, and 641 (Figure 1). hSGLT1 and its two mutants, W561hSGLT1 and W0hSGLT1, were expressed in *P. pastoris* and purified to homogeneity with yields of ∼3, 2.5, and 1.5 mg/L of culture, respectively. Proteins were more than 95% pure as judged by Coomassie staining and Western blot analysis with an anti-FLAG antibody (Figure 2). As observed previously, the apparent molecular mass of the transporter is ∼55 kDa, suggesting a lack of glycosylation of the protein (*8*).

Transport Properties of Proteoliposomes Containing hSGLT1, W561hSGLT1, and W0hSGLT1 in the Presence or Absence of Na^+. In Figure 3, the uptake of α-MDG by proteoliposomes containing hSGLT1, W561hSGLT1, or W0hSGLT1 is shown. hSGLT1 proteoliposomes take up

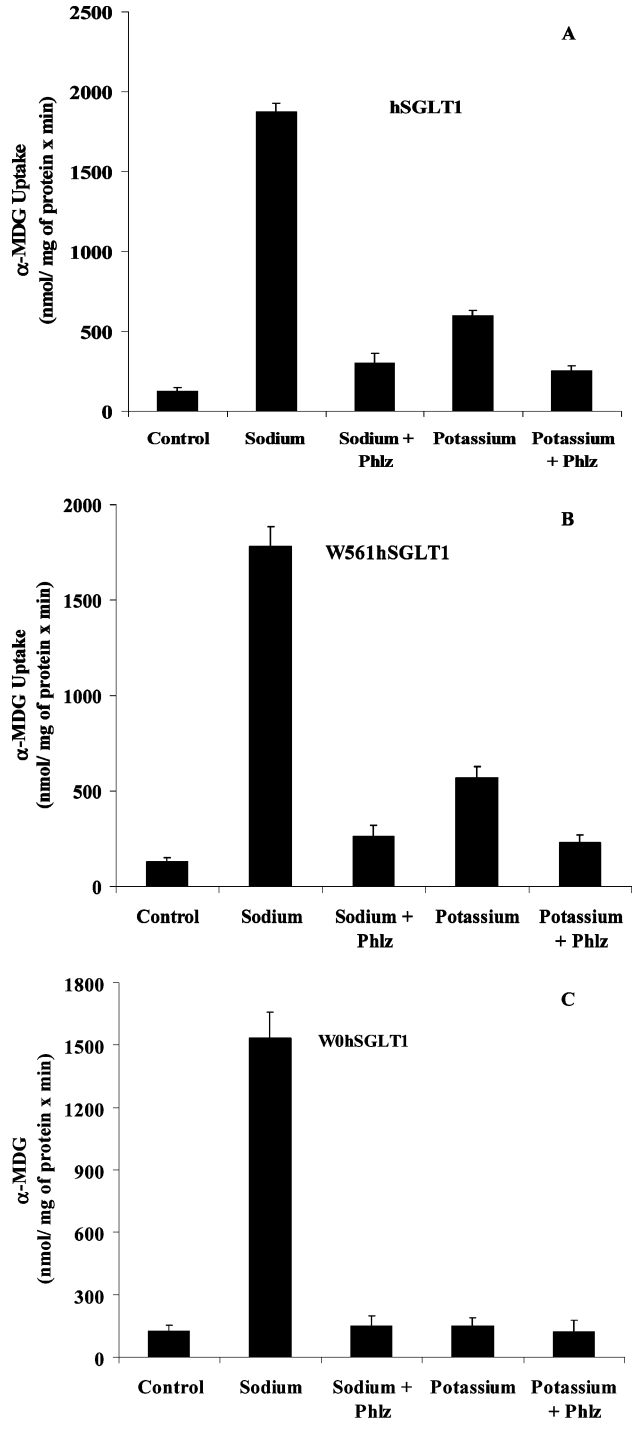

FIGURE 3: Sugar uptake characteristics of proteoliposomes containing purified recombinant hSGLT1, W561hSGLT1, or W0hSGLT1. (A) Uptake of 50 μM α-MDG by proteoliposomes made of purified hSGLT1: 1874 ± 55 nmol (mg of protein)$^{-1}$ min^{-1} in the presence of 100 mM Na^+ and 598 ± 36 nmol (mg of protein)$^{-1}$ min^{-1} in the presence of 100 mM K^+. Phlorizin (10 μM) inhibited sugar transport up to 251 ± 39 nmol (mg of protein)$^{-1}$ min^{-1}, whereas liposomes (control) transported only 125 ± 20 nmol (mg of lipid)$^{-1}$ min^{-1}. (B) W561hSGLT1 shows a 5% decrease in the level of uptake of α-MDG in the presence of Na^+ [1780 ± 103 nmol (mg of protein)$^{-1}$ min^{-1}] or K^+ [570 ± 58 nmol (mg of protein)$^{-1}$ min^{-1}], whereas phlorizin exerts the same effect on transport. (C) In W0hSGLT1, the level of Na^+-dependent transport decreases by 14% to a value of 1535 ± 123 nmol (mg of protein)$^{-1}$ min^{-1} and K^+-dependent transport was almost completely abolished.

Table 1: Apparent α-MDG Affinities of hSGLT1, W561hSGLT1, and W0hSGLT1 Reconstituted in Proteoliposomes[a]

	K_m (mM)	
protein	with Na^+	with K^+
hSGLT1	0.40 ± 0.05	3.5 ± 0.17
W561hSGLT1	0.43 ± 0.08	3.2 ± 0.2
W0hSGLT1	0.54 ± 0.11	NA[b]

[a] The level of α-MDG uptake was measured at various α-MDG concentrations (0.01−10 mM for hSGLT1 and W561hSGLT1 and 0.01−50 mM for W0hSGLT1). K_m values were determined using the equation $V = V_{max} + [S]/(K_{0.5} + [S])$, where [S] is the sugar concentration, V_{max} the maximal velocity for a saturating [S], and $K_{0.5}$ the apparent affinity constant. [b] The transport was completely abolished; see the text for details.

1874 ± 55 nmol (mg of protein)$^{-1}$ min^{-1} in the presence of 100 mM Na^+ as compared to 125 ± 20 nmol (mg of liposomes)$^{-1}$ min^{-1} by liposomes alone. Sodium-dependent α-MDG uptake was completely blocked by 100 μM phlorizin. Proteoliposomes containing hSGLT1 also exhibited a higher level of α-MDG uptake than liposomes when sodium was replaced with potassium [598 ± 36 nmol (mg of protein)$^{-1}$ min^{-1}], and this uptake was also strongly inhibited by 100 μM phlorizin.

Proteoliposomes composed of W561hSGLT1 (devoid of 13 of its native Trps) exhibit an only 5% decrease in the level of α-MDG uptake in the presence of Na^+ or K^+ as compared to hSGLT1-containing proteoliposomes. In the tryptophan-free W0hSGLT1-containing proteoliposomes, the level of α-MDG uptake in the presence of sodium decreased by 14% to a value of 1535 ± 123 nmol (mg of protein)$^{-1}$ min^{-1}, while sodium-independent phlorizin inhibitable α-MDG uptake was completely abolished. These results suggest that none of the 14 Trp residues in hSGLT1 is essential for the sodium-dependent transport function, while the Trp residue at position 561 plays a critical role in sodium-independent transport activity. The specificity of sugar uptake by hSGLT1, W561hSGLT1, and W0hSGLT1 in proteoliposomes in the presence of 100 mM Na^+ or K^+ was measured by assessing the inhibition of uptake at 100 μM α-MDG by 10 mM D-glucose (D-Glc), D-galactose (D-Gal), D-mannose (Man), D-allose (All), and L-glucose (L-Glc) and 100 μM phlorizin (Phlz) (data not shown). All three proteins exhibit the following order of substrate specificity: α-MDG > D-Glc ≈ D-Gal ≫ All > Man. Also, with respect to stereospecificity, all three preferred D-Glu over L-Glu. For the determination of kinetic parameters, 1 min α-MDG uptake assays were performed at varying α-MDG concentrations from 0.01 to 20 mM in the presence of 100 mM Na^+ or K^+. Half-saturation constants (*12*) of 0.40 ± 0.05 mM for hSGLT1, 0.43 ± 0.08 mM for W561hSGLT1, and 0.54 ± 0.11 mM for W0hSGLT1 were obtained in the presence of Na^+. In the absence of Na^+, the K_m values for hSGLT1 and W561hSGLT1 were ∼5−6-fold higher (Table 1).

Ligand-Induced Changes in the Steady-State Fluorescence of Reconstituted hSGLT1 in the Absence of Na^+. The emission spectrum of native hSGLT1 reconstituted in proteoliposomes exhibited a broad maximum at 338−340 nm (Figure 4A), indicating that the majority of Trp residues of hSGLT1 responsible for fluorescence are located in a relatively nonpolar environment. The effects of sugars and inhibitors on the intrinsic fluorescence in the absence of Na^+

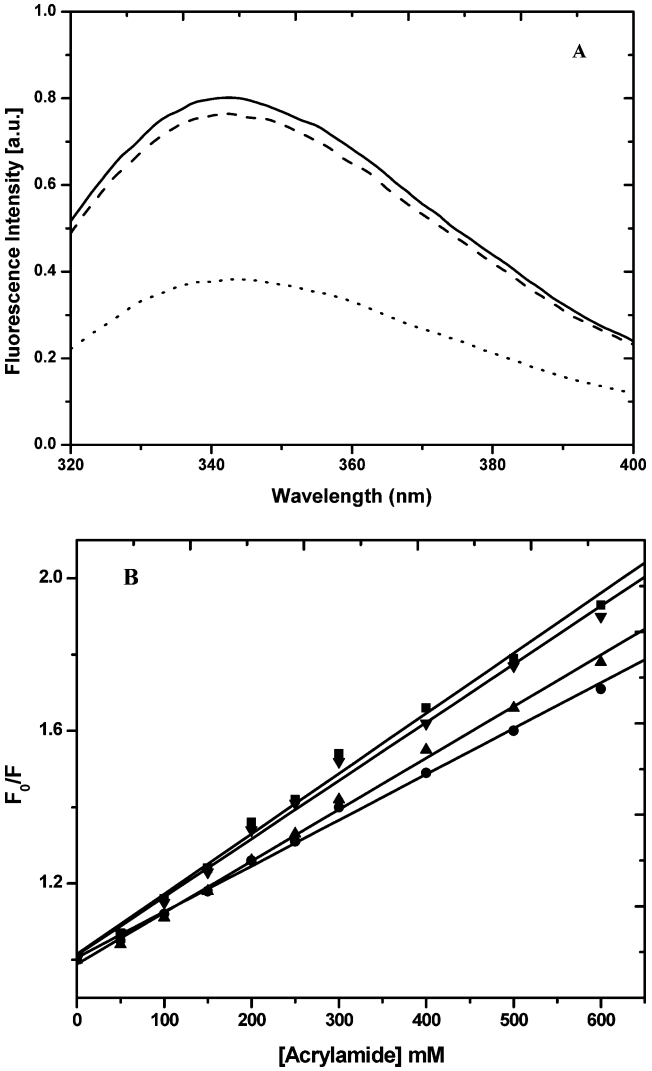

FIGURE 4: Effect of D-glucose or phlorizin on the corrected emission spectrum of hSGLT1 and Stern−Volmer plots of Trp fluorescence quenching by acrylamide in the presence of 100 mM K^+. (A) For each experiment, 1 μM hSGLT1 reconstituted into proteoliposomes at a ratio of 200:1 was incubated in the absence (—) or presence of 10 mM D-glucose (- - -) or in the presence of 100 μM phlorizin (···). The excitation wavelength was 295 nm. The results shown are typical of ≈20 independent experiments. All of the spectra were corrected as described in Experimental Procedures; a.u. stands for arbitrary units. (B) Acrylamide alone (■), 10 mM D-glucose (●), 100 μM phlorizin (▲), or 100 μM phloretin (▼). Quenching experiments were performed as described in Experimental Procedures. The slopes of the best-fit linear regression lines for each data set (K_{SV} values) are listed in Table 3. The mean ± standard deviation of three independent experiments are given. No difference in quenching was observed for L-Trp.

are compiled in Table 2. In the presence of K^+, α-MDG, D-glucose, D-galactose, and phlorizin decreased the Trp fluorescence of hSGLT1 by 8, 6, 5.5, and 50%, respectively (Figure 4A and Table 2). Other sugars also affected Trp fluorescence but to a lesser extent; noteworthy is the fact that in the presence of L-glucose hSGLT1 does not show any change in fluorescence. The K_d values calculated for sugars by fluorescence quenching are in the order α-MDG, D-glucose, D-galactose, 6-deoxy-D-glucose, 2-deoxy-D-glucose, and allose with values of 3.4 ± 0.5, 3.8 ± 0.35, 3.9 ± 0.2, 9.5 ± 1.0, 9.8 ± 1.0, and 17 ± 1.5 mM, respectively. Binding affinities calculated for hSGLT1 in the presence of K^+ are 5−6-fold lower than the values obtained previously in the presence of Na^+ by monitoring fluorescence changes and by measuring transport activities (*8*).

KI, Acrylamide, and TCE Trp Fluorescence Quenching of Reconstituted hSGLT1 in the Absence or Presence of D-Glucose or Phlorizin in a Sodium-Free Solution. Fluorescence quenching has been used widely to study the relative accessibility of fluorescent groups in membrane proteins. Ionic quenchers provide information about the polarity and/or electrostatic properties of the milieu in the vicinity of the fluorophore, and neutral quenchers provide information about steric hindrance. In Figure 4B, the titration curve with acrylamide is shown. Acrylamide as well as KI and TCE (data not shown) exhibited linear Stern−Volmer relationships. In the absence of ligand, the quenching constant for KI was 1.11 M^{-1}, for acrylamide 1.49 M^{-1}, and for TCE 1.98 M^{-1} (Figure 4B and Table 3). In the presence of D-glucose or phlorizin, all three quenchers exhibited less quenching (Table 3); the decrease in quenching was more prominent in the presence of D-glucose than in the presence of phlorizin. These data confirm that some Trp residues are critically involved in the sodium-independent, phlorizin inhibitable sugar binding/translocation site of the cotransporter and that D-glucose and phlorizin provide protection against KI, acrylamide, or TCE quenching. To further investigate which part of the glucoside phlorizin, the sugar moiety or the aglucone, is responsible for this protection effect, we performed hSGLT1 quenching experiments in the presence of phloretin. We could not observe any protection effect when we used 100 μM phloretin (Figure 4B and Table 3).

Ligand-Induced Changes in the Steady-State Fluorescence of W561hSGLT1 Reconstituted in Proteoliposomes in the Absence of Na^+. The corrected spectrum of the intrinsic Trp fluorescence of W561hSGLT1 is shown in Figure 5. The emission spectrum is narrower than that of hSGLT1 with a maximum at ≈343 nm and slightly shifted to the red, indicating that the remaining Trp at position 561 is solvated with water. Importantly, addition of D-glucose decreased the fluorescence by 10% with a blue shift of 2−4 nm, while phlorizin did so with a 50% decrease in fluorescence with a more prominent blue shift of 8−10 nm in the emission maxima in a highly reproducible fashion. Effects of different ligands on W561hSGLT1 fluorescence were assessed quantitatively and are compiled in Table 2. The most interesting aspect of these results is that the wild type and W561hSGLT1 behave almost identically and that the sugars exhibit a change in Trp fluorescence according to their affinity found in the transport studies.

KI, Acrylamide, and TCE Quenching of Trp Fluorescence of W561hSGLT1 Reconstituted in Proteoliposomes in the Absence or Presence of D-Glucose or Phlorizin in a Sodium-Free Solution. The environment surrounding Trp-561 was further studied by fluorescence quenching. The water-soluble ion I^- was used as a collisional quencher to probe the solvent accessibility of Trp-561 in the absence or presence of D-glucose, phlorizin, or phloretin. Acrylamide and TCE, another collisional quencher, were also tested (Table 3) to investigate possible electrostatic effects of I^-. All experimental data fit linear Stern−Volmer plots for collisional (dynamic) quenching, thereby excluding a contribution from static quenching. In the absence of all three ligands, the K_{SV}

Table 2: Effect of Ligands on the Trp Fluorescence of hSGLT1 and W561hSGLT1 in Proteoliposomes in the Presence of K^+

	change in fluorescence[a] (%)		shifts in maxima		K_d[b] (mM)	
ligand	hSGLT1	W561hSGLT1	hSGLT1	W561hSGLT1	hSGLT1	W561hSGLT1
α-MDG	−8.0 ± 1	−10.0 ± 1.0	2−4 (blue)	2−4 (blue)	3.4 ± 0.5	3.2 ± 0.3
D-glucose	−6.0 ± 1	−9.0 ± 1.0	2−4 (blue)	2−4 (blue)	3.8 ± 0.35	3.3 ± 0.5
D-galactose	−5.5 ± 0.5	−7.5 ± 0.5	2−4 (blue)	2−4 (blue)	3.9 ± 0.20	3.6 ± 0.22
6-deoxy-D-glucose	−3.5 ± 0.2	−4.0 ± 0.3	no	no	9.5 ± 1.0	9.1 ± 1.2
2-deoxy-D-glucose	−3.0 ± 0.2	−3.5 ± 0.1	no	no	9.8 ± 1.0	9.5 ± 1.0
D-allose	−1.0 ± 0.2	−1.5 ± 0.1	no	no	17.0 ± 1.5	15.5 ± 2.0
D-mannose	no change	no change	no	no	ND[c]	ND[c]
L-glucose	no change	no change	no	no	ND[c]	ND[c]
phlorizin	−50.0 ± 5.0	−50.0 ± 5.0	4−6 (blue)	8−10 (blue)	0.005 ± 0 0.0008	0.005 ± 0.0008

[a] A negative sign indicates fluorescence quenching after addition of ligand. [b] The apparent equilibrium dissociation constant (K_d) were determined from the nonlinear regression analysis of the percentage of fluorescence quenching as a function of ligand concentration using a computer-based analysis program (Prism). Values are the mean ± standard deviation of three independent experiments. [c] Not determined.

Table 3: Stern−Volmer Quenching Constants (K_{SV}) of hSGLT1 and W561hSGLT1 in the Absence or Presence of D-Glucose or Phlorizin and in the Presence of K^+[a]

	K_{SV} (M^{-1}) in the absence of ligand[b]		K_{SV} (M^{-1}) in the presence of 10 mM D-glucose[c]		K_{SV} (M^{-1}) in the presence of 100 μM phlorizin[d]		K_{SV} (M^{-1}) in the presence of 100 μM phloretin[e]	
quencher	hSGLT1	W561hSGLT1	hSGLT1	W561hSGLT1	hSGLT1	W561hSGLT1	hSGLT1	W561hSGLT1
KI	1.11 ± 0.04	2.25 ± 0.05	0.89 ± 0.03	1.14 ± 0.03	1.02 ± 0.03	1.78 ± 0.05	1.14 ± 0.03	2.19 ± 0.05
acrylamide	1.49 ± 0.05	2.86 ± 0.06	1.21 ± 0.04	1.46 ± 0.03	1.32 ± 0.03	2.04 ± 0.04	1.47 ± 0.04	2.85 ± 0.05
TCE	1.98 ± 0.05	3.69 ± 0.15	1.54 ± 0.04	2.62 ± 0.11	1.69 ± 0.05	3.23 ± 0.11	1.93 ± 0.05	3.67 ± 0.19

[a] The Stern−Volmer quenching constants were determined from the slopes of the lines from the equation $F_0/F = 1 + K_{SV}[Q]$. Values are the mean ± standard deviation of three independent experiments. [b] Quenching experiments were conducted in the absence of ligand. [c] Quenching experiments were conducted in the presence of 10 mM D-glucose. [d] Quenching experiments were conducted in the presence of 100 μM phlorizin. [e] Quenching experiments were conducted in the presence of 100 μM phloretin.

values obtained for all three quenchers reflect an accessibility of Trp-561 to solvent (Table 3) higher than that of the bulk tryptophans in wild-type hSGLT1. Importantly, there is a significant reduction of the K_{SV} values for all three quenchers in the presence of D-glucose (50, 49, and 29% for KI, acrylamide, and TCE, respectively) or phlorizin (21, 29, and 13% for KI, acrylamide, and TCE, respectively), providing further evidence that Trp-561 is shielded from the surrounding solvent by substrate. In the presence of phloretin, i.e., the aglucone moiety of phlorizin (Table 3) or L-glucose (data not shown), no reduction in the K_{SV} values of KI, acrylamide, or TCE was observed.

DISCUSSION

Transport Studies. hSGLT1, W561hSGLT1, and W0hSGLT1 bearing a C-terminal histidine tag and FLAG tag at amino acid position 574 were expressed and purified from *P. pastoris*. All three proteins are functional as judged by sodium-stimulated, secondary active sugar (α-MDG) uptake (Figure 3). After mutation of 13 Trps native in hSGLT1 to Phe in W561hSGLT1, in this mutant the rate of sodium-dependent or potassium-dependent transport decreased by 5% and the K_m value of the W561 mutant was almost identical to that of the wild-type protein. These results clearly indicate that those 13 Trp residues do not play very significant roles in sugar or inhibitor interaction or sugar translocation. Similar results were reported for the lactose permease of *Escherichia coli* (*13*), where mutation of five of six native Trps did not affect the activity of the transporter. In the mutant W0hSGLT1 (devoid of all its native Trp residues), the rate of sodium-dependent transport decreased slightly, but sodium-independent phlorizin inhibitable transport was completely abolished. The decrease in the level of uptake in the presence of sodium [341 nmol (mg of protein)$^{-1}$ min^{-1}] is almost as large as the level of sodium-independent phlorizin inhibitable uptake [473 nmol (mg of protein)$^{-1}$ min^{-1}]. This might suggest that the sodium-dependent and sodium-independent pathways can be used in parallel at the low α-MDG concentration used in the uptake experiments, as predicted from earlier kinetic considerations (*10*). The change in the sodium-independent uptake indicates that the Trp residue at position 561 plays a critical role in sodium-independent sugar interaction and/or transport. This assumption is supported by blue shifts in the emission maxima observed for W561hSGLT1 in the presence of D-glucose or phlorizin. This shift likely represents a change in the polarity of the local environment of Trp561, resulting from hydrophobic stacking between the glucopyranoside ring of sugar and the indole ring of Trp561, thereby excluding water molecules from the side chain. The presence of Trp residues in the sugar binding sites for different transporter proteins has been reported in previous studies (*14*−*19*).

Fluorescence Studies. Fluorescence studies of hSGLT1 and W561hSGLT1 reconstituted into proteoliposomes provide further evidence that Trp-561 in hSGLT1 forms part of a low-affinity sugar binding/translocation site which is independent of sodium. In the Trp fluorescence studies of hSGLT1 in the presence of K^+, we observed an opposite response as compared to its fluorescence changes in the presence of Na^+ (*8*). The Trp fluorescence in this case decreased rather than increased in the presence of different ligands. The apparent affinity constants calculated in the presence of K^+ are higher by a factor of 5−6 than the values calculated in the presence of Na^+, except for that of phlorizin binding which has a comparable affinity in both cases (Table 2). These data suggest a different conformation of the

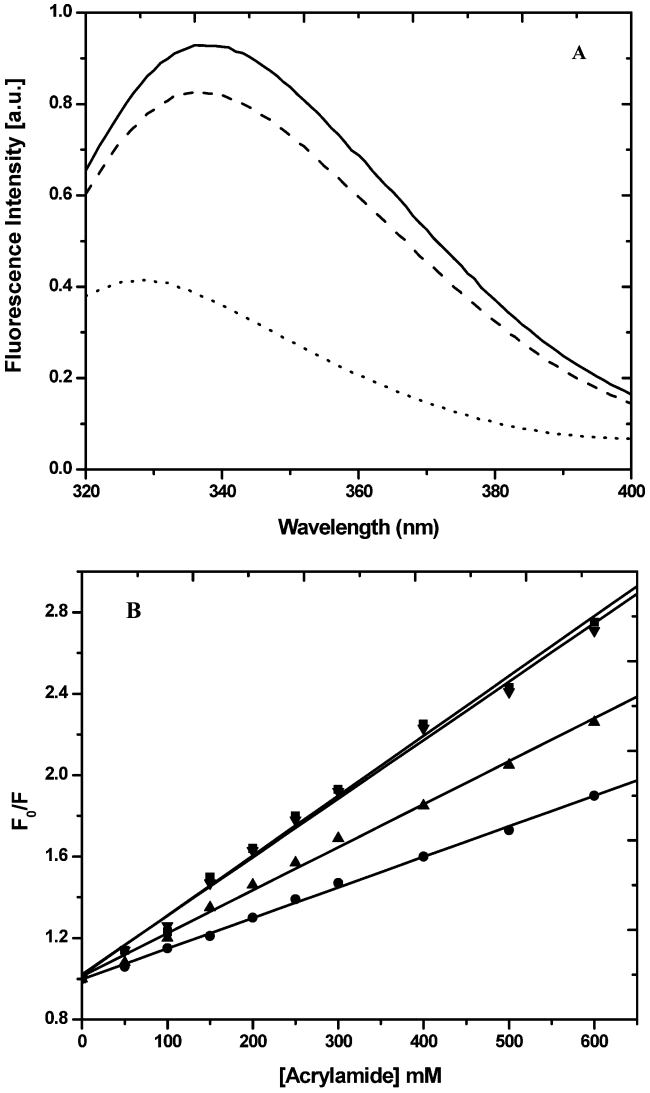

FIGURE 5: Effect of D-glucose or phlorizin on the corrected emission spectrum of W561hSGLT1 in the presence of 100 mM K^+ and Stern−Volmer plot for fluorescence quenching by acrylamide. (A) For each experiment, 1 μM W561hSGLT1 reconstituted into proteoliposomes at a ratio of 200:1 was incubated in the absence (—) or presence of 10 mM D-glucose (- - -) or in the presence of 100 μM phlorizin (···). The excitation wavelength was 295 nm. The results shown are typical of ≈20 independent experiments. All of the spectra were corrected as described as in Experimental Procedures; a.u. stands for arbitrary units. (B) Acrylamide alone (■), 10 mM D-glucose (●), 100 μM phlorizin (▲), or 100 μM phloretin (▼). K_{SV} values are given in Table 3.

(sodium-free) glucose−carrier complex than of the carrier saturated with sodium and D-glucose. This assumption is further supported by Trp fluorescence quenching by KI, acrylamide, or TCE in the presence of D-glucose (Table 3). In the absence of sodium, we observed a significant protection effect against all quenchers with a decrease in the level of quenching with smaller K_{SV} values. In the presence of sodium, the fluorescence tended to increase (*8*). To investigate which part of phlorizin, the sugar moiety or the aglucone part, is responsible for this protection effect, phloretin was used as a ligand; in this case, we could not observe any protection effect against quenching. These data clearly demonstrate that the sugar moiety of phlorizin is responsible for this protection effect. To further trace the location of this low-affinity sugar binding/translocation site in hSGLT1, we constructed the W561 mutant of hSGLT1 which contains a single Trp residue at position 561, with all other 13 Trp residues being mutated to Phe. Trp fluorescence properties of this mutant show a shift of the maximum to the right as expected from the preponderance of the signal of a Trp located in a hydrophilic environment. The effects of different ligands on Trp fluorescence and apparent affinities calculated for the W561 mutant of hSGLT1 were essentially the same as those calculated for hSGLT1 in the presence of potassium. The most striking difference was the much larger protection effect of D-glucose and phlorizin against KI, acrylamide, or TCE quenching, underlining the essential role of Trp-561 as part of the low-affinity D-glucose binding site. That there is a sodium-independent low-affinity binding site located around Trp-561 is also suggested by results obtained by our group in AFM studies on isolated loop 13 (B. Wimmer et al., unpublished results), and Trp fluorescence studies on truncated loop 13 from amino acids 541−598 (M. M. Raja et al., unpublished results). For the direct mapping of the low-affinity sugar binding site, we performed photolabeling of hSGLT1, W561hSGLT1, and loop 13 protein with different analogues of D-glucose (*20*) in sodium phosphate or potassium phosphate buffer, but we were not able to detect any labeling. These negative results might be due to the low affinity of this binding site for sugars or the low labeling efficiency. When we mutated W561 to tyrosine instead of phenylalanine, mutant Y561hSGLT1 exhibited kinetic parameters essentially similar to those of the W0hSGLT1 mutant (data not shown). This result supports the assumption that W561 is critical for low-affinity sodium-independent D-glucose binding and/or transport. To check for the presence of W561 in SGLT1 known from other species and different isoforms of human SGLT, we performed sequence alignments with ClustalW (Figure 6). To our surprise, W561 is conserved in all known SGLT1 isoforms in different species except *Vibrio parahaemolyticus* vSGLT1 (*21*). In different isoforms of human SGLT, W561 is also conserved except for hSGLT3, which contains Phe at this position; a consequence of the absence of Trp at this position might be that hSGLT3 works as a glucose sensor but not as a glucose transporter (*22*). This high degree of conservation suggests that Trp-561 represents an essential element for the cotransporter. The same holds for the existence of leak pathways in which sodium-independent translocation of sugars can occur (*10*). For effective energetic coupling, these pathways have to be small compared to the sodium−glucose cotransport, but they are required for thermodynamic reasons. The data given above characterize such a pathway at the molecular level in a, be it artificial but, precisely defined experimental system, where only the cotransporter protein contributes to the observed signals. The stereospecificity which is almost identical to the one observed in the presence of sodium would suggest that a glucose binding site at the outside of the carrier is studied; similarly, the interaction with phlorizin supports this conclusion (*23*, *24*).

SGLT1 in Vitro versus Sugar Transport in Vivo. The studies reported above were performed with recombinant isolated hSGLT1 reconstituted into proteoliposomes. Such studies always raise several questions. One is the orientation of the transporter after reconstitution. We think that hSGLT1 in the proteoliposomes is predominantly oriented right-side-

```
A  Human          IPDVHLYRLCWSLRNSKEERIDLDA-EEENIQEGPKETIEIETQVPEKKK 599
   Mice           IPDVHLYRLCWSLRNSKEERIDLDAGEEEDIPEDSKDTIEIDTEAPQKKK 600
   Rat            IPDVHLYRLCWSLRNSTEERIDLDAGEEEPVEEDPKDTIEIDAEAPQKEK 600
   Cow            IADVHLYRLCWSLRNSKEERIDLDA-EDEDVQDAREDALEIDTEASEEKK 599
   Rabbit         IPDVHLYRLCWSLRNSKEERIDLDA-GEEDIQEAPEEAT--DTEVPKKKK 597
   Sheep          IADVHLYRLCWSLRNSKEERIDLDAEDEDIQDAREDALEIDTEAS      595
   Dogfish        IDDIHLYRLCWTLRHSTEKREDLDSDDWNNQDN-DSKMDVDEESP      595
   Pig            PAGVQIENLTW--------------------------------        549
   Vibrio         LSTS---------------------------------------------- 502
B  hSGLT1         PTIICGVHYLYFAIILFAISFITIVVISLLTKPIPDVHLYRLCWSLRNS- 566
   hSGLT2         PKIICGVHYLYFSIVLFFGSMLVTLGISLLTKPIPDVHLYRLCWVLRNS- 566
   hSGLT3         PAFLCGVHYLYFAIVLFFCSGLLTLTVSLCTAPIPRKHLHRLVFSLRHS- 566
   hSGLT4         PVLVKSIHYLYFSMILSTVTLITVSTVSWFTEPPSKEMVSHLTWFTRHDP 498
   hSGLT5         PAVLKDFHYLYFAILLCGLTAIVIVIVSLCTTPIPEEQLTRLTWWTRNCP 589
   hSGLT6         PAVLGSIHYLHFAVALFALSGAVVVAGSLLTPPPQSVQIENLTWWT---- 520
```

FIGURE 6: Amino acid sequence alignment of SGLT1 isoforms from different species and SGLTs from humans. The highly conserved Trp is highlighted in bold. Sequences are identified with the NCBI accession numbers in parentheses, and sequence alignment was performed using ClustalW (http://www.ebi.ac.uk/clustalw). (A) Known SGLT1 isoforms from different species: human, *H. sapiens* SGLT1 (NP_000334); mouse, *Mus musculus* SGLT1 (AAF17249); rat, *Rattus norvegicus* SGLT1 (NP_037165); cow, *Bos taurus* SGLT1 (AAM34274); rabbit, *Oryctolagus cuniculus* SGLT1 (P11170); sheep, *Ovis aries* SGLT1 (P53791); dogfish, *Squalus acanthias* SGLT1 (CAJ75582); and Vibrio, *V. parahaemolyticus* SGLT (AAF80602). (B) Different isoforms of SGLT from humans: hSGLT1, *H. sapiens* SGLT1 (NP_000334); hSGLT2, *H. sapiens* SGLT2 (NP_003032); hSGLT3, *H. sapiens* SGLT3 (NP_055042); hSGLT4, *H. sapiens* SGLT4 (NP_001011547); hSGLT5, *H. sapiens* SGLT5 (NP_689564); and hSGLT6, *H. sapiens* SGLT6 (NP_443176).

out on the basis of the following. First, the sodium-independent transport is inhibited by phlorizin, an inhibitor shown in a variety of experimental systems to interact only with the outside of the transporter. This interaction can also occur in the absence of sodium since in phlorizin binding studies sodium lowers the affinity for the high-affinity binding site, but this is not an absolute requirement for the binding (*25*). Since binding of phlorizin involves both the hydrophobic aglucone part and sugar moiety (*26*), even at a low sugar affinity of the transporter binding of phlorizin can occur, probably mainly guided by the interactions with hydrophobic amino acids located in outside-oriented loops. The exact location of these remains a matter of discussion (*23*, *27*−*29*). There is also further evidence of the right-side-out orientation of the transporter in the proteoliposomes from digestion experiments with trypsin beads. These studies demonstrated by subsequent mass spectrometry that only peptides were generated which according to topology models are present in loops at the outside of the transporter (A. Kumar et al., manuscript submitted for publication). Second, there is always the possibility that there might be partial uncoupling of the transporter due to the lipids that are used or the procedure employed for reconstitution. Lipids indeed can play a significant role in transport activity, as previously shown by Da Cruz et al. (*30*), for example, but the strongest evidence of sodium-independent phlorizin inhibitable glucose flux was initially obtained in brush border membrane vesicles, where no reconstitution is necessary and the native phospholipids are present (*10*). What might be missing in all in vitro studies, however, are the membrane- and transporter-associated proteins that have been found in in vivo studies. Similarly, posttranslational modifications such as glycosylation or phosphorylation might be absent, thus changing the properties of the transporter. This hypothesis might explain why sodium-independent sugar fluxes mediated by hSGLT1 are not observed to a significant extent in intact cells but can be demonstrated in these studies on purified hSGLT1 containing proteoliposomes and in previous studies on isolated brush border membranes (*10*). In summary, this study provides the first conclusive evidence based on transport studies and Trp fluorescence studies on the isolated hSGLT1 and its two mutants that hSGLT1 contains a second low-affinity D-glucose binding and translocation site and that Trp-561 forms part of this binding site which is independent of sodium. These data clearly demonstrate the presence of sugar leak pathways in SGLT1 at a molecular level; how these are regulated in the intact cell in vivo remains to be elucidated.

REFERENCES

1. Hediger, M. A., Coady, M. J., Ikeda, T. S., and Wright, E. M. (1987) Expression cloning and cDNA sequencing of the Na^+/glucose co-transporter, *Nature 330*, 379−381.
2. Loo, D. D., Hirayama, B. A., Gallardo, E. M., Lam, J. T., Turk, E., and Wright, E. M. (1998) Conformational changes couple Na^+ and glucose transport, *Proc. Natl. Acad. Sci. U.S.A. 95*, 7789−7794.
3. Meinild, A. K., Loo, D. D., Hirayama, B. A., Gallardo, E., and Wright, E. M. (2001) Conformational changes couple Na^+ and glucose transport, *Biochemistry 40*, 11897−11904.
4. Panayotova-Heiermann, M., Loo, D. D., Kong, C. T., Lever, J. E., and Wright, E. M. (1996) Sugar binding to Na^+/glucose cotransporters is determined by the carboxyl-terminal half of the protein, *J. Biol. Chem. 271*, 10029−10034.
5. Panayotova-Heiermann, M., Eskandari, S., Turk, E., Zampighi, G. A., and Wright, E. M. (1997) Five transmembrane helices form

the sugar pathway through the Na^+/glucose cotransporter, *J. Biol. Chem. 272*, 20324−20327.
6. Diez-Sampedro, A., Wright, E. M., and Hirayama, B. A. (2001) Residue 457 controls sugar binding and transport in the Na^+/glucose cotransporter, *J. Biol. Chem. 276*, 49188−49194.
7. Diez-Sampedro, A., Loo, D. D., Wright, E. M., Zampighi, G. A., and Hirayama, B. A. (2004) Coupled sodium/glucose cotransport by SGLT1 requires a negative charge at position 454, *Biochemistry 43*, 13175−13184.
8. Tyagi, N. K., Goyal, P., Kumar, A., Pandey, D., Siess, W., and Kinne, R. K. (2005) High-yield functional expression of human sodium/D-glucose cotransporter1 in *Pichia pastoris* and characterization of ligand-induced conformational changes as studied by tryptophan fluorescence, *Biochemistry 44*, 15514−15524.
9. Firnges, M. A., Lin, J. T., and Kinne, R. K. (2001) Functional asymmetry of the sodium-D-glucose cotransporter expressed in yeast secretory vesicles, *J. Membr. Biol. 179*, 143−153.
10. Centelles, J. J., Kinne, R. K. H., and Heinz, E. (1991) Energetic coupling of Na-glucose cotransport, *Biochim. Biophys. Acta 1065*, 239−249.
11. Ikeda, T. S., Hwang, E. S., Coady, M. J., Hirayama, B. A., Hediger, M. A., and Wright, E. M. (1989) Characterization of a Na^+/glucose cotransporter cloned from rabbit small intestine, *J. Membr. Biol. 110*, 87−95.
12. Verkman, A. S., Lukacovic, M. F., Tinklepaugh, M. S., and Dix, J. A. (1986) Quenching of red cell tryptophan fluorescence by mercurial compounds, *Membr. Biochem. 6*, 269−289.
13. Menezes, M. E., Roepe, P. D., and Kaback, H. R. (1990) Design of a membrane transport protein for fluorescence spectroscopy, *Proc. Natl. Acad. Sci. U.S.A. 87*, 1638−1642.
14. Vazquez-Ibar, J. L., Guan, L., Svrakic, M., and Kaback, H. R. (2003) Exploiting luminescence spectroscopy to elucidate the interaction between sugar and a tryptophan residue in the lactose permease of *Escherichia coli*, *Proc. Natl. Acad. Sci. U.S.A. 100*, 12706−12711.
15. Vazquez-Ibar, J. L., Guan, L., Weinglass, A. B., Verner, G., Gordillo, R., and Kaback, H. R. (2004) Sugar recognition by the lactose permease of *Escherichia coli*, *J. Biol. Chem. 279*, 49214−49221.
16. Abramson, J., Smirnova, I., Kasho, V., Verner, G., Kaback, H. R., and Iwata, S. (2003) Structure and mechanism of the lactose permease of *Escherichia coli*, *Science 301*, 610−615.
17. Kasahara, T., and Kasahara, M. (1998) Tryptophan 388 in putative transmembrane segment 10 of the rat glucose transporter Glut1 is essential for glucose transport, *J. Biol. Chem. 273*, 29113−29117.
18. Garcia, J. C., Strube, M., Leingang, K., Keller, K., and Mueckler, M. M. (1992) Amino acid substitutions at tryptophan 388 and tryptophan 412 of the HepG2 (Glut1) glucose transporter inhibit transport activity and targeting to the plasma membrane in *Xenopus* oocytes, *J. Biol. Chem. 267*, 7770−7776.
19. Martineau, P., Szmelcman, S., Spurlino, J. C., Quiocho, F. A., and Hofnung, M. (1990) Genetic approach to the role of tryptophan residues in the activities and fluorescence of a bacterial periplasmic maltose-binding protein, *J. Mol. Biol. 214*, 337−352.
20. Tyagi, N. K., and Kinne, R. K. (2003) Synthesis of photoaffinity probes [2′-iodo-4′-(3″-trifluoromethyldiazirinyl)phenoxy]-D-glucopyranoside and [(4′-benzoyl)phenoxy]-D-glucopyranoside for the identification of sugar-binding and phlorizin-binding sites in the sodium/D-glucose cotransporter protein, *Anal. Biochem. 323*, 74−83.
21. Turk, E., Kim, O., le Coutre, J., Whitelegge, J. P., Eskandari, S., Lam, J. T., Kreman, M., Zampighi, G., Faull, K. F., and Wright, E. M. (2000) Molecular characterization of *Vibrio parahaemolyticus* vSGLT: A model for sodium-coupled sugar cotransporters, *J. Biol. Chem. 275*, 25711−25716.
22. Diez-Sampedro, A., Hirayama, B. A., Osswald, C., Gorboulev, V., Baumgarten, K., Volk, C., Wright, E. M., and Koepsell, H. (2003) A glucose sensor hiding in a family of transporters, *Proc. Natl. Acad. Sci. U.S.A. 100*, 11753−11758.
23. Raja, M. M., Tyagi, N. K., and Kinne, R. K. (2003) Phlorizin recognition in a C-terminal fragment of SGLT1 studied by tryptophan scanning and affinity labeling, *J. Biol. Chem. 278*, 49154−49163.
24. Wielert-Badt, S., Hinterdorfer, P., Gruber, H. J., Lin, J. T., Badt, D., Wimmer, B., Schindler, H., and Kinne, R. K. (2002) Single molecule recognition of protein binding epitopes in brush border membranes by force microscopy, *Biophys. J. 82*, 2767−2774.
25. Kinne, R. (1976) Properties of the glucose transport system in the renal brush border membrane, *Curr. Top. Membr. Transp. 8*, 209−267.
26. Wielert-Badt, S., Lin, J. T., Lorenz, M., Fritz, S., and Kinne, R. K. (2000) Probing the conformation of the sugar transport inhibitor phlorizin by 2D-NMR, molecular dynamics studies, and pharmacophore analysis, *J. Med. Chem. 43*, 1692−1698.
27. Xia, X., Lin, J. T., and Kinne, R. K. (2003) Binding of phlorizin to the isolated C-terminal extramembranous loop of the Na^+/glucose cotransporter assessed by intrinsic tryptophan fluorescence, *Biochemistry 42*, 6115−6120.
28. Gagnon, D. G., Holt, A., Bourgeois, F., Wallendorff, B., Coady, M. J., and Lapointe, J. Y. (2005) Membrane topology of loop 13−14 of the Na^+/glucose cotransporter (SGLT1): A SCAM and fluorescent labelling study, *Biochim. Biophys. Acta 1712*, 173−184.
29. Novakova, R., Homerova, D., Kinne, R. K., Kinne-Saffran, E., and Lin, J. T. (2001) Identification of a region critically involved in the interaction of phlorizin with the rabbit sodium-D-glucose cotransporter SGLT1, *J. Membr. Biol. 184*, 55−60.
30. Da Cruz, M. E., Kinne, R., and Lin, J. T. (1983) Temperature dependence of D-glucose transport in reconstituted liposomes, *Biochim. Biophys. Acta 732*, 691−698.

BI061696X